Received: 23 November 2022 | Revised: 31 July 2023 | Accepted: 5 October 2023

DOI: 10.1002/asjc.3258

SPECIAL ISSUE ARTICLE

WILEY

Properties of interconnected negative imaginary systems and extension to formation-containment control of networked multi-UAV systems with experimental validation results

Yu-Hsiang Su[1] | **Parijat Bhowmick**[2] | **Alexander Lanzon**[1]

[1]Department of Electrical and Electronic Engineering, University of Manchester, Manchester, UK

[2]Department of Electronics and Electrical Engineering, Indian Institute of Technology Guwahati, Assam, India

Correspondence
Yu-Hsiang Su, Department of Electrical and Electronic Engineering, University of Manchester, Manchester, UK.
Email: yu-hsiang.su@manchester.ac.uk

Funding information
This research was supported by the Engineering and Physical Sciences Research Council (EPSRC) (grant number EP/R008876/1) and by the Science and Engineering Research Board (SERB), DST, India (grant number SRG/2022/000892). All research data supporting this publication are directly available within this publication. For the purpose of open access, the authors have applied a Creative Commons Attribution (CC BY) license to any Author Accepted Manuscript version arising.

Abstract

This paper extends the properties of a positive feedback interconnection of two negative imaginary (NI) systems to multi-agent NI systems and proposes a new formation-containment control methodology relying on the characteristic loci technique. Inspired by recent applications of NI and passivity-based control techniques in the multi-agent systems (MAS) domain, a new formation-tracking and containment control scheme is developed for a class of networked multi-UAV systems. The proposed scheme offers a two-stage and two-loop control configuration where the inner loop uses a cascaded PID controller to ensure stable hovering of the UAVs, and the outer loop deploys a distributed "mixed" SNI and strictly passive controller to achieve the formation-containment objectives. This scheme works with a dynamic output feedback control strategy; hence, it offers advantages when the full-state measurement is not possible. In contrast to the well-known Lyapunov theory-based cooperative control schemes, the present one exploits the characteristic loci technique to prove the formation-tracking and containment phenomena theoretically. The paper also provides experimental validation results on a fleet of Crazyflie 2.1 nano quadcopters.

KEYWORDS

characteristics loci, consensus, formation-containment control, multi-UAV systems, negative imaginary systems, positive feedback

1 | INTRODUCTION

Negative imaginary (NI) systems theory, first presented in Lanzon and Petersen [1], was a new development in the broad area of robust control, parallel to passivity theory [2]. It was initially motivated by the principle of "position control of inertial systems via positive feedback" [3], which is common in systems with collocated position sensors (or acceleration sensors) and force actuators [1, 4]. NI dynamics are highly correlated to the notion of counter-clockwise input-output (I/O) systems [5], I/O Hamiltonian systems [6] and a new type of dissipative systems defined with respect to the input (u) and time-derivative of the system's output ($\dot{y}$) [7, 8]. Various potential applications of the NI theory include large space structures [3], robotic manipulators [9], networked

multi-agent systems [10–13], nano-positioning systems [14], and so on.

NI theory has become attractive due to its simple closed-loop stability criterion that relies on the systems' gains only at $\omega = 0$. Lanzon and Petersen [1] first established that a positive feedback loop containing a stable NI and a strictly NI (abbreviated as SNI) system remains asymptotically stable if the product of the systems' gains at $\omega = 0$ is smaller than one (defined as the *DC loop gain* criterion). Later, Xiong et al. [15] showed that this stability criterion equally applies to the case when one of the systems has poles on the $j\omega$-axis except at $s = 0$. It has been further generalised to allow NI systems to have a maximum of two poles at $s = 0$ [9, 16–18].

Over the last two decades, cooperative control of multi-agent systems (MASs) has been a promising research domain within the control and robotics communities. This field encompasses different types of coordinated control problems, such as leader-following consensus, formation-tracking, containment, formation-containment, rendezvous, flocking, herding, and so on. Among them, the formation-containment control (FCC) action involves formation-tracking of the leader agents and containment control of the follower agents [19, 20]. Liu et al. [21] did the pioneering research in developing an FCC scheme for MASs. After that, Chen et al. [22] proposed an adaptive formation-containment control scheme for networked Euler–Lagrange systems. Not only FCC but the entire cooperative control literature has been flourishing gracefully, with recent developments drawing significant attention. For instance, Chen et al. [23] investigated the leader-follower affine formation maneuver control for high-order multi-agent systems; Liang et al. [24] proposed a bipartite consensus tracking methodology applying a fuzzy-based fault-tolerant control approach; Liang et al. [25] addressed the consensus control problem with power integrators using a neuro-adaptive approach; and Su et al. [26] proposed a new robust adaptive formation controller for muti-UAV systems that can be applied to cooperative payload transportation missions. These advancements showcase the vibrant and dynamic nature of the cooperative control field. Since 2015, the NI theory has found practical applications in the development of cooperative control laws for MASs, including multi-robot and multi-UAV systems [27–29]. Previous articles [13, 30] established the theoretical foundation for NI-based cooperative control schemes. Later, V. P. Tran et al. exploited the results of previous articles [13, 30] in developing various formation control configurations for multi-quadcopter systems (see the survey paper Tran et al. [31] and the references cited therein). In parallel, Skeik et al. [12] designed an NI-based rendezvous control scheme for a group of feedback-linearized two-wheeled mobile robots. More recently, previous works [10, 11] have come up with NI-based cooperative control schemes for single-integrator MASs, with their theoretical proofs relying on the properties of *characteristic loci* (also known as *eigenvalue loci*) of NI systems [32].

Drawn by a consistent urge to expand the scope of NI theory-based cooperative control and improve its performance, this paper has designed a distributed FCC scheme for a class of multi-UAV systems utilizing the notion of "mixed" SNI + strictly passive system property and characteristic loci technique. Below, we summarize the main contributions of this paper and the salient features of the proposed FCC scheme:

- This paper has introduced a two-stage and two-loop formation-containment control scheme for a class of multi-UAV systems whose translational dynamics can be modeled as a double-integrator MAS. Stage 1 and Stage 2 (see Figure 2) represent formation-tracking and containment control, respectively. The two-loop control configuration (see Figure 7b) consists of an inner loop that deploys a cascaded PID controller to ensure stable hovering and an outer loop that contains a distributed control protocol for achieving the FCC (formation-tracking and containment control) objectives.
- A "mixed" SNI + strictly passive FCC protocol is designed that offers a better dynamic and steady-state performance compared to the SNI-only scheme (e.g., [11–13, 31]). Besides, the scheme works with both negative and positive feedback.
- This FCC scheme relies on dynamic output feedback, making it a suitable choice for applications where full-state feedback is unavailable. Moreover, this scheme applies to both single and double-integrator NI MASs.
- The proposed FCC protocol does not use any nonlinear or switching functions, unlike many existing well-known cooperative control schemes [19, 33–37] that result in a *discontinuous* control action and, in turn, suffer from the *chattering* effect.
- In contrast to the well-established Lyapunov theory-based FCC schemes [19, 22, 23, 33, 38–40], the proposed methodology exploits the characteristic loci technique to derive the theoretical proof. It helps to reduce the theoretical complexity (Theorem 5) and facilitates straightforward implementation.
- The proposed FCC scheme also takes care of topology switching and network reconfiguration, offers robustness to any stable unstructured uncertainty in additive/multiplicative form and to a sudden loss of agents.
- The paper has tested the feasibility and performance of the proposed FCC scheme through two indoor multi-UAV experiments. These experiments were

conducted on a group of Crazyflie 2.1 nano quadcopters to achieve i) a formation-containment control mission and ii) a time-varying formation-tracking mission (refer to Sections 6.3 and 6.4).

Apart from the main contribution to developing a two-stage and two-loop FCC scheme for multi-UAV systems, the paper has also discussed the properties of a positive feedback interconnection of NI systems allowing poles on the imaginary axis including the origin (refer to Section 3).

Notation and symbols

The notation and acronyms are standard throughout. $\mathbb{R}$ and $\mathbb{C}$ denote the sets of real and complex numbers respectively. The set of all $(m \times n)$ real matrices are denoted by $\mathbb{R}^{m\times n}$. A^* denotes the complex conjugate transpose of a matrix A while $A^\top$ indicates the transpose of a matrix. The symbol $(A^{-1})^*$ is used as a shorthand for A^{-*} when exists. $(\cdot)'$ represents the transpose of a vector. For a matrix A having only real eigenvalues, $\lambda_{\max}(A)$ stands for its maximum eigenvalue. $R^{\sim}(s)$ indicates the adjoint of a transfer function matrix $R(s)$ given by $R^\top(\bar{s})$ where $\bar{s}$ denotes the complex-conjugate of s. $R(j\omega)^* = R(-j\omega)^\top$ is noted for a transfer function matrix $R(s)$. $\mathcal{RH}_\infty^{m\times m}$ is the space containing all proper, real, rational and stable transfer functionmatrices with $m \times m$ dimension. $R(s) = \left[\begin{array}{c|c} A & B \\ \hline C & D \end{array}\right]$ signifies a minimal state-space description of a proper, real, rational transfer function matrix $R(s)$. Let $\mathbf{1}_n$ be the column vector with all n entries equal to 1. The Kronecker product of two matrices A and B is denoted by $A \otimes B$. $\|.\|$ expresses the 2-norm of a vector or a matrix.

2 | TECHNICAL BACKGROUND AND PROBLEM FORMULATION

2.1 | Preliminaries of NI theory

This subsection reviews the frequency-domain definitions of NI and SNI systems. Afterwards, it presents a state-space characterization for NI systems without imposing any minimality condition.

Definition 1 (NI system [9, 18]. Let R be a square, dynamical LTI system with a proper, real, rational transfer function matrix $R(s)$. Then, $R(s)$ is called an NI system if

- $j[R(j\omega) - R(j\omega)^*] \geq 0 \quad \forall \omega \in (0,\infty)$ except the values of ω where $s = j\omega$ is a pole of $R(s)$.
- If $s = j\omega_0$ with $\omega_0 \in (0,\infty)$ is a pole of $R(s)$, then it is at most a simple pole and the residue matrix $\lim_{s\to j\omega_0}(s - j\omega_0)jR(s)$ is Hermitian and positive semidefinite.
- If $s = 0$ is a pole of $R(s)$, then $\lim_{s\to 0} s^k R(s) = 0$ for all $k \geq 3$ and $\lim_{s\to 0} s^2 R(s)$ is Hermitian and positive semidefinite.

Definition 2 (SNI system [1]. Let R be a square, dynamical, asymptotically stable, LTI system with a proper, real, rational transfer function matrix $R(s) \in \mathcal{RH}_\infty^{m\times m}$. Then, $R(s)$ is called an SNI system if $j[R(j\omega) - R(j\omega)^*] > 0$ $\forall \omega \in (0,\infty)$.

We will now present a state-space characterization for NI systems with possible poles on the $j\omega$ axis, including the origin.

Lemma 1 (Bhowmick et al. [41]. Let R be a square, LTI, dynamical system with a proper, real, rational transfer function matrix $R(s)$ and a state-space description $\left[\begin{array}{c|c} A & B \\ \hline C & D \end{array}\right]$. Then,

1. R is NI if $D = D^\top$ and there exists a $P = P^\top$ such that

$$\begin{bmatrix} PA + A^\top P & PB - A^\top C^\top \\ B^\top P - CA & -(CB - B^\top C^\top) \end{bmatrix} \leq 0; \tag{1}$$

2. there exists a $P = P^\top \geq 0$ satisfying (1) and $D = D^\top$ if R is NI and $\left[\begin{array}{c|c} A & B \\ \hline C & D \end{array}\right]$ does not have any observable but uncontrollable modes.

We now recall the following Lemma, which gives a criterion for a system to become NI with poles on the $j\omega$ axis excluding $s = 0$.

Lemma 2 (Lanzon and Chen [18]. Suppose $R(s)$ is NI. Choose a negative definite matrix Ψ that satisfies $\lambda_{\max}[R(\infty)\Psi] < 1$. Then, $R_1(s) = R(s)[I - \Psi R(s)]^{-1}$ is NI without any pole at $s = 0$.

Lemma 2 states that, under certain technical assumptions, the closed-loop system interconnection comprised of $R(s)$ and Ψ, via positive feedback, exhibits the NI property.

With reference to Lemma 2, the next Lemma shows the existence of a positive definite matrix $\overline{P}$ that can be described in terms of $R(s)$ and Ψ. In essence, Lemma 3 extends Lemma 2.

Lemma 3 (Bhowmick et al. [41]. Suppose $R(s)$ is an NI system with a minimal state-space description $\left[\begin{array}{c|c} A & B \\ \hline C & D \end{array}\right]$. We select a $\Psi < 0$ satisfying the condition $\lambda_{\max}[R(\infty)\Psi] < 1$. Then $\overline{P} = P - C^\top \Psi(I - D\Psi)^{-1}C > 0$ where $P = P^\top \geq 0$ satisfies (1).

Then, in Lemma 4, we show that the positive definite matrix $\overline{P}$ is a solution of the LMI conditions given in (2).

Lemma 4 (Bhowmick et al. [41]. Suppose the assumptions of Lemma 3 hold, and furthermore, let $R_1(s) = R(s)[I - \Psi R(s)]^{-1}$ have a minimal state-space description $\left[\begin{array}{c|c} \bar{A} & \bar{B} \\ \hline \bar{C} & \bar{D} \end{array}\right]$ with $\bar{A} = A + B\Psi(I - D\Psi)^{-1}C$, $\overline{B} = B(I - \Psi D)^{-1}$, $\overline{C} = (I - D\Psi)^{-1}C$ and $\overline{D} = D(I - \Psi D)^{-1}$.Then, $\overline{D} = \overline{D}^\top$, $\det(\bar{A}) \neq 0$ and $\overline{P} = P - C^\top \Psi(I - D\Psi)^{-1}C > 0$ satisfies

$$\bar{A}\overline{P}^{-1} + \overline{P}^{-1}\bar{A}^\top \leq 0 \text{ and } \overline{B} + \bar{A}\overline{P}^{-1}\overline{C}^\top = 0 \tag{2}$$

where $P = P^\top \geq 0$ is a solution of (1).

To this end, we will present the closed-loop stability theorem for an NI-SNI interconnection without imposing any restrictions on the systems' gains at $\omega = \infty$, which in turn makes the loop strictly proper.

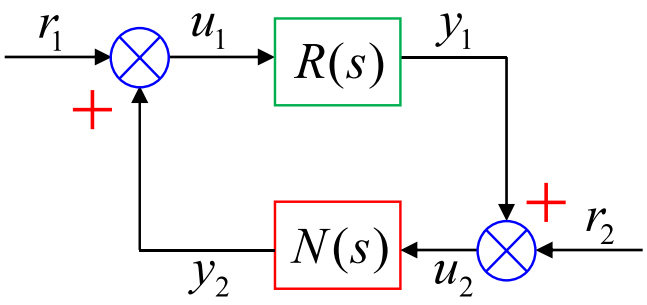

FIGURE 1 Two NI systems $R(s)$ and $N(s)$ are connected via a positive feedback.

Theorem 1 (NI-SNI stability theorem without poles at the origin **[18].** Consider an NI system $R(s)$ without poles at $s = 0$ and an SNI system $N(s)$. Then the positive feedback closed-loop system comprised of $R(s)$ and $N(s)$, shown in Figure 1, is asymptotically stable if and only if

$$\begin{cases} \det[I - R(\infty)N(\infty)] \neq 0, \\ \lambda_{\max}\left[(I - R(\infty)N(\infty))^{-1}(R(\infty)N(0) - I)\right] < 0, \\ \lambda_{\max}\left[(I - N(0)R(\infty))^{-1}(N(0)R(0) - I)\right] < 0. \end{cases} \tag{3}$$

The readers are referred to Lanzon and Chen [18] for results when $R(s)$ contains poles at $s = 0$.

2.2 | Passivity and "mixed" NI + passive systems

After discussing the NI theory, we will now review the definitions of passive and strictly passive systems.

Definition 3 (Passive system **[2].** A system $G(s) \in \mathcal{R}^{m\times m}$ with no RHP poles is called passive if $G(j\omega) + G(j\omega)^* \geq 0 \ \forall \omega \in \mathbb{R}$ except those $\omega_0 \in \omega$ where $s = j\omega_0$ is a pole of $G(s)$. The multiplicity of the pole $s = j\omega_0$ cannot be more than one and the residue matrix $\Delta|_{s=j\omega_0} \triangleq \lim_{s\to j\omega_0}(s - j\omega_0)G(s) = \Delta|^*_{s=j\omega_0} \geq 0$.

Definition 4 (Strictly passive system **[2][1].** A system $G(s) \in \mathcal{RH}_\infty^{m\times m}$ is called strictly passive if $G(j\omega) + G(j\omega)^* > 0 \ \forall \omega \in \mathbb{R}$.

Ultimately, we would like to put forward a new class of LTI systems that exhibits a "mixed" SNI and strictly passive property. Originally, Patra and Lanzon [42] proposed the notion of "mixed" NI + finite-gain system property and later, Das et al. [43] defined a class of "mixed" NI + finite-gain + passive systems along the direction of Patra and Lanzon [42]. According to previous works [42, 43], a system is called "mixed" SNI + strictly passive if it exhibits the SNI property in some frequency intervals and the strictly passive property

[1]For detailed classification of strictly passive systems, please refer to Desoer and Vidyasagar [2].

in others. For example, $G_1(s)=\frac{(s+1)}{(s+6)(s^2+4s+8)}$, $G_2(s)=\frac{s+1}{(s^2+8s+32)}$, $G_3(s)=\frac{s+1}{(s+10)^3}$, and so on.

Definition 5 ("Mixed" SNI + strictly passive property**.** Let $G(s)\in\mathcal{RH}_\infty^{m\times m}$ be the transfer function matrix of a dynamical system G. Suppose $[G(s)+G^{\sim}(s)]$ and $[G(s)-G^{\sim}(s)]$ both have full normal rank m. Let

$$\begin{aligned}\Omega_1 &= \{\omega\in(0,\infty): j[G(j\omega)-G(j\omega)^*]>0 \text{ and } [G(j\omega)+G(j\omega)^*]\not\geq 0\}\\ \Omega_2 &= \{\omega\in(0,\infty): j[G(j\omega)-G(j\omega)^*]>0 \text{ and } [G(j\omega)+G(j\omega)^*]>0\}\\ \Omega_3 &= \{\omega\in(0,\infty): j[G(j\omega)-G(j\omega)^*]\not\geq 0 \text{ and } [G(j\omega)+G(j\omega)^*]>0\}\end{aligned}$$

Then, $G(s)$ is said to have a "mixed" SNI + strictly passive property if Ω_1, Ω_2 and Ω_3 are non-empty sets satisfying $\Omega_1\cup\Omega_2\cup\Omega_3=(0,\infty)$ and $G(s)$ is strictly passive at $\omega=0$.

2.3 | Graph theory

A group of networked agents exchanges information with each other via a communication topology. In this work, we used a weighted undirected graph $\mathcal{G}=\{\mathcal{V},\mathcal{E},\mathcal{A}\}$ to describe the communication topology among each agent. Here, $\mathcal{V}=\{1,...,N\}$ denotes the node set, $\mathcal{E}\subset\mathcal{V}\times\mathcal{V}$ represents the edge set, and $\mathcal{A}=[a_{ij}]\in\mathbb{R}^{N\times N}$ is the associated adjacency matrix. The edge $e_{ji}=(v_j,v_i)\in\mathcal{E}$ indicates that information is transmitted from node j to node i. The weight a_{ij} corresponds to the weight of e_{ji}, and $a_{ij}>0$ if $e_{ji}\in\mathcal{E}$. The in-degree matrix is defined as $\mathcal{D}=\text{diag}\{d_i\}\in\mathbb{R}^{N\times N}$, where $d_i=\sum_{j=1}^{N}a_{ij}$. The Laplacian matrix $\mathcal{L}\in\mathbb{R}^{N\times N}$ of $\mathcal{G}$ is defined as $\mathcal{L}=\mathcal{D}-\mathcal{A}$. If the ith agent is connected to a virtual leader or target (labeled as "k"), an edge e_{ki} is said to exist between them with a pinning gain $p_i>0$.

2.4 | Properties of multi-agent NI systems

We will now mention an important property that needs to be satisfied by a networked multi-agent NI system.

Property 1. The communication topology among the N homogeneous NI agents is described by an undirected and connected graph $\mathcal{G}$. A root node (the virtual target) always exists that directly provides reference trajectory to one or multiple connected agents.

Owing to Property 1, the graph Laplacian matrix enjoys the property $(\mathcal{L}+\mathbb{P})>0$ in the homogeneous case, where $\mathbb{P}=\text{diag}\{p_1,p_2,\cdots,p_N\}>0$ is the pinning-gain matrix. The element p_i for $i\in\{1,2,\cdots,N\}$ in $\mathbb{P}$ represents the weight of the interaction edge connecting a root node and the ith agent. The following Lemma proves that a homogeneous multi-agent NI (or SNI) system satisfying Property 1 retains the NI (or SNI) property. The concept was first proved in Wang et al. [13] and has since been used in many other papers.

Lemma 5 (Wang et al. [13]. Consider a homogeneous multi-agent NI (or SNI) system with Property 1. Then, $\overline{M}(s)=(\mathcal{L}+\mathbb{P})\otimes M(s)$ is NI (or SNI) $\Leftrightarrow$ $M(s)$ is NI (or SNI).

Lemma 6 shows that a network of all homogeneous stable NI (including SNI) systems retains the same sign definiteness of its DC-gain matrix when the corresponding communication topology satisfies Property 1.

Lemma 6. Consider a network of N identical stable NI agents $M(s)\in\mathcal{RH}_\infty^{N\times N}$ satisfying Property 1. Denote $\overline{M}(s)=(\mathcal{L}+\mathbb{P})\otimes M(s)$. Then, $\overline{M}(0)>0$ (resp. <0) if and only if $M(0)>0$ (resp. <0).

2.5 | Characteristic loci theory

The concept of *characteristic loci* and its application in determining the closed-loop asymptotic stability of LTI MIMO systems were introduced by MacFarlane and Belletrutti during the period of 1969–1973 [44, 45]. This concept is analogous to a *multi-loop* Nyquist criterion that offers a pretty convenient graphical stability analysis tool for MIMO systems. The characteristic loci $\lambda_i(s)$, where $i\in\{1,2,...,m\}$, of any square LTI system $\Sigma(s)\in\mathcal{R}^{m\times m}$ are obtained through a conformal mapping of the complex function $\det[\Sigma(s)]$ into another complex plane when s follows the standard s-plane D-contour in a clockwise (CW) direction (see Figure 3a).

Theorem 2 ([44, 45]. A necessary and sufficient criterion for a closed-loop interconnection of two LTI systems $\Sigma(s)$ and $\Sigma_c(s)$,

connected via negative feedback, to maintain asymptotic stability is that the total number of the counter-clockwise (CCW) encirclements about the $(-1+j0)$ point by the characteristic loci $\lambda_i(j\omega)$ of $L(s) \triangleq \Sigma(s)\Sigma_c(s)\ \forall i \in \{1,2,...,n\}$ should be equal to the number of right-half plane (RHP) poles of $L(s)$. When $L(s) \in \mathcal{RH}_\infty^{m\times m}$, none of the characteristic loci $\lambda_i(j\omega)$ should encircle the $(-1+j0)$ point.

2.6 | Problem statement

Given a multi-UAV system whose translational dynamics can be modeled as a double integrator multi-agent system, the primary objective is to design a two-stage and two-loop formation-containment control (FCC) scheme (see Figure 7b) of which the inner loop applies a cascaded PID control block to ensure a stable hovering of the UAVs and the outer loop deploys a distributed dynamic output feedback formation-containment controller exploiting a "mixed" NI plus passivity approach. The second objective is to validate the proposed FCC scheme on a group of real-world quadcopter UAVs.

3 | PROPERTIES OF INTERCONNECTED NI SYSTEMS

This section presents the results from our previous work in Bhowmick et al. [41], which will serve as the basis for developing a new distributed dynamic output feedback FCC scheme in Section 4.

3.1 | Properties of a positive feedback NI interconnection allowing poles at the origin

Theorem 3 proposes a set of "if and only if" criteria required for an NI interconnection, constructed via positive feedback, allowing poles on the $j\omega$ axis, including $s=0$ to preserve the NI property.

Theorem 3 (Bhowmick et al. [41]. Suppose $R(s)$ and $N(s)$ are NI systems. Choose $\Psi_1<0$ and $\Psi_2<0$ such that $\lambda_{\max}[N(\infty)\Psi_1]<1$ and $\lambda_{\max}[\Psi_2(R(\infty)-\Psi_1)]<1$. Then, the input-output transfer function mapping from $\begin{bmatrix} r_1 \\ r_2 \end{bmatrix}$ to $\begin{bmatrix} y_1 \\ y_2 \end{bmatrix}$, designated by $\Sigma(s)$, is NI and has no poles at $s=0$ (resp. $\det\left(\lim_{s\to 0}\left[[R(\infty)N(s)-I][I-\Psi_1 N(s)]^{-1}\right]\right)\neq 0$) if and only if

$$\det[I-R(\infty)N(\infty)]\neq 0,$$
$$\lambda_{\max}\left[\lim_{s\to 0}[[I-\Psi_1 N(\infty)][I-R(\infty)N(\infty)]^{-1}[R(\infty)N(s)-I][I-\Psi_1 N(s)]^{-1}]\right]<0 \text{ and}$$
$$\lambda_{\max}\left[\lim_{s\to 0}[[I-\Psi_2(R(\infty)-\Psi_1)][I-N(s)R(\infty)]^{-1}[N(s)R(s)-I][I-\Psi_2(R(s)-\Psi_1)]^{-1}]\right]<0 (\text{resp.}\leq 0).$$

3.2 | Properties of an NI interconnection with possible $j\omega$-axis poles excluding $s=0$

Theorem 4 gives a set of "if and only if" criteria for a positive-feedback interconnection of two NI systems (refer to Figure 1), allowing poles on the imaginary axis (excluding the origin) to maintain the NI property in closed-loop.

Theorem 4 (Bhowmick et al. [41]. Suppose $R(s)$ and $N(s)$ are NI systems with no poles at $s=0$. Then, the input-output transfer function mapping from $\begin{bmatrix} r_1 \\ r_2 \end{bmatrix}$ to $\begin{bmatrix} y_1 \\ y_2 \end{bmatrix}$, designated by $\Sigma(s)$, is NI and has no pole(s) at $s=0$ (resp. $\det(I-R(\infty)N(0))\neq 0$) if and only if

$$\begin{cases} \det[I-R(\infty)N(\infty)]\neq 0, \\ \lambda_{\max}\left[(I-R(\infty)N(\infty))^{-1}(R(\infty)N(0)-I)\right]<0, \\ \lambda_{\max}\left[(I-N(0)R(\infty))^{-1}(N(0)R(0)-I)\right]<0 \\ \qquad (\text{resp. } \leq 0). \end{cases}$$

4 | A "MIXED" SNI PLUS STRICT PASSIVITY-BASED FORMATION-CONTAINMENT CONTROL SCHEME

This section presents the key developments of this paper. A distributed dynamic output feedback formation-containment control (FCC) scheme is built for a class of multi-agent systems, with a specific focus on applications to multi-UAV systems. The dynamics/kinematics of these systems can be approximated by a group of double integrator NI agents connected via an undirected graph. The proposed scheme exploits a new strategy of "mixed" SNI + strictly passive cooperative control law instead of the "NI only" cooperative control laws used in the existing

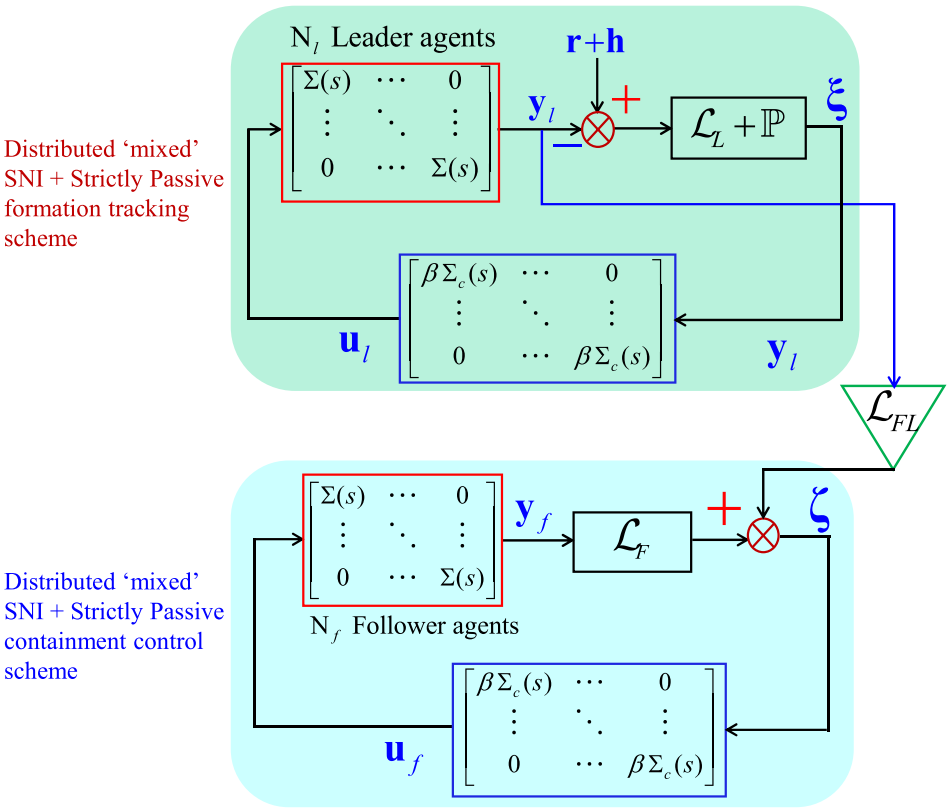

FIGURE 2 A formation-containment control scheme for a networked multi-agent/multi-UAV system involving distributed "mixed" SNI + strictly passive controllers.

literature [10–13,30,31]. Furthermore, to the best of our knowledge, this is the first paper in the NI literature that addresses the formation-tracking and containment control problem while also introducing the concept of a "mixed" SNI + strictly passive cooperative control scheme for a class of multi-agent/multi-UAV systems.

We consider a homogeneous multi-UAV system consisting of N_l leaders and N_f followers. This paper aims to achieve two primary control objectives: (i) formation (static/time-varying) tracking of the leader agents surrounding a virtual target; and (ii) containment of the follower agents. Although the present work addresses a single group formation-tracking problem, it can be readily extended to a multi-group formation-tracking problem, considering multiple targets to track. The closed-loop translational dynamics of the UAVs can be approximated by a decoupled three-input-three-output double integrator system that, by default, exhibits the NI property with a double pole at $s = 0$. This fact inspires us to apply NI theory to develop a distributed dynamic output feedback FCC scheme for multi-UAV systems. A two-loop control configuration is employed in practical implementation, as depicted in Figure 7b. The inner-loop controller, which can be a single/cascaded PID controller, a sliding-mode controller, or a back-stepping controller, is responsible for maintaining stable hovering of the UAVs. The distributed FCC protocol serves as the outer-loop controller, enabling coordinated formation-containment control of the UAVs. In the present case, the graph Laplacian matrix of the overall network can be expressed in the partitioned form as $\mathscr{L} = \left[\begin{array}{c|c} \mathscr{L}_L & 0 \\ \hline \mathscr{L}_{FL} & \mathscr{L}_F \end{array}\right]$ where $\mathscr{L}_L \in \mathbb{R}^{N_l \times N_l}$, $\mathscr{L}_F \in \mathbb{R}^{N_f \times N_f}$ and $\mathscr{L}_{FL} \in \mathbb{R}^{N_f \times N_l}$.

We will now mention a few crucial properties that the network topology $\mathcal{G}$ of the multi-UAV system should satisfy.

Property 2. In the case of an undirected graph topology, the leaders should be well-connected. At least one leader should be directly connected to the virtual target (treated as the root node). In the case of a directed graph, there must exist a spanning tree from the root node.

Property 3. The followers are also well-connected, and at least one leader must exist for each follower that has a directed path to that follower.

Property 4. The leaders cannot receive information from the followers. Leaders and followers rely on the output information of their neighbors only, but not on the information of all agents.

As a consequence of Property 2, for an undirected graph, $(\mathscr{L}_L+\mathbb{P})>0$ and for directed cases, $(\mathscr{L}_L+\mathbb{P})$ qualifies as an M-matrix. Owing to Property 3, the rows of the matrix $-\mathscr{L}_F^{-1}\mathscr{L}_{FL}$ have a row-sum equal to 1. This result is well-known in matrix theory and is related to algebraic graphs [19]. We are now ready to state the main Theorem of this paper, which provides the theoretical basis of the projected "mixed" SNI + strictly passive FCC scheme for networked multi-UAV systems.

Theorem 5. Given a homogeneous NI multi-UAV system consisting of N_l leaders and N_f followers whose simplified closed-loop translational dynamics (in each channel) are given by $\Sigma(s)=\frac{1}{s^2}$. Suppose the associated network topology $\mathcal{G}$ satisfies Properties 2–4. Choose a "mixed" SNI + strictly passive controller $\Sigma_c(s)\in\mathcal{RH}_\infty$ with $\Sigma_c(0)>0$ for the scheme shown in Figure 2. Let $\mathbf{r}=\mathbf{1}_{N_l}r$ denote the position of the virtual target and $\mathbf{h}=\begin{bmatrix}h_{l_1} & h_{l_2} & \cdots & h_{l_{N_l}}\end{bmatrix}^\top$ is the desired formation configuration vector. Then, there always exists a finite $\beta\in(0,\beta^\star]$ such that the multi-UAV system achieves the formation-containment objectives (i.e., formation-tracking and containment control) by the following distributed dynamic output feedback control law

$$u_i=\beta\Sigma_c(s)\sum_{j=1}^{N_l}a_{ij}\Big((y_i-h_i)-\big(y_j-h_j\big)\Big)+p_i(y_i-h_i-r)\quad\forall i\in\{l_1,l_2,\ldots,l_{N_l}\}\tag{4}$$

$$\text{and } u_k=\beta\Sigma_c(s)\sum_{j=1}^{N_l+N_f}a_{kj}\big(y_k-y_j\big)\quad\forall k\in\{f_1,f_2,\ldots,f_{N_f}\}.\tag{5}$$

Proof. The proof has been divided into two parts: **Part I** is dedicated to the formation-tracking and **Part II** establishes the containment control technique.

Part I: Formation-tracking of N_l leader UAVs The closed-loop control scheme shown at the top of Figure 2 is responsible for formation-tracking, which has the loop transfer function $T_L=(\mathscr{L}_L+\mathbb{P})\otimes\frac{1}{s^2}\Sigma_c(s)$. The symbol $\bar{\lambda}_i(s)$ represents the characteristic loci of T_L where $i\in\{l_1,l_2,\ldots,l_{N_l}\}$. To proceed with the proof, three sets Ψ_0, $\Psi_{\pm\jmath}$ and Ψ_∞ of the Laplace variable s are defined corresponding to three specific regions marked (as shown in Figure 3a) along the standard s-plane D-contour. To prove the asymptotic stability of the proposed formation-tracking scheme, we will exploit the characteristic loci theorem (Theorem 2). This proof consists of the following three cases.

Case I: For the subset $s\in\Psi_0$ We can approximately express the characteristic loci $\bar{\lambda}_i(s)$

$$\bar{\lambda}_i(s)|_{s\in\Psi_0}=\lambda_i[(\mathscr{L}_L+\mathbb{P})\otimes\Sigma_c(0)]\frac{1}{\varepsilon^2}e^{-j2\theta}\tag{6}$$

where λ_i simply denotes the ith eigenvalue of a real matrix. Let $\lambda_i[(\mathscr{L}_L+\mathbb{P})\otimes\Sigma_c(0)]=c_ie^{j\phi_i}$ where $\phi_i=0\ \forall i$ since $\Sigma_c(0)>0$ and $(\mathscr{L}_L+\mathbb{P})>0$. Then, (6) takes the form $\bar{\lambda}_i(s)|_{s\in\Psi_0}=\frac{c_i}{\varepsilon^2}e^{j(\phi_i-2\theta)}$. Therefore, $\bar{\lambda}_i(j0_+)=$

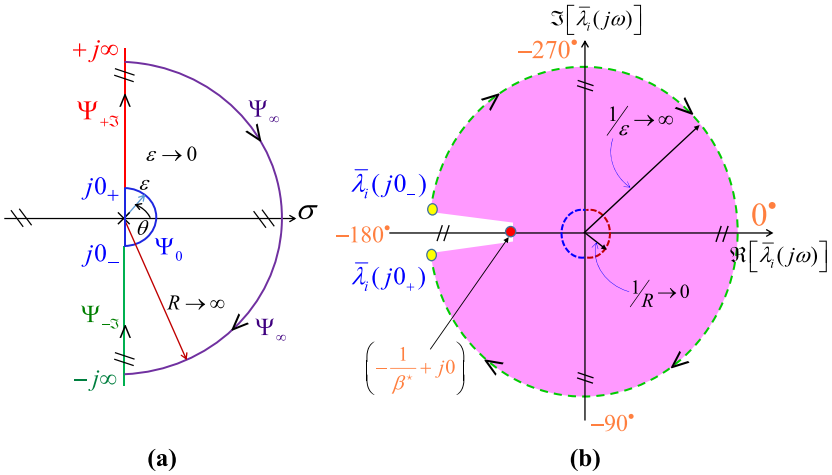

FIGURE 3 (a) The standard s-plane Nyquist $\mathcal{D}$-contour. (b) All the characteristic loci $\bar{\lambda}_i(s)$ of $(\mathscr{L}_L+\mathbb{P})\otimes\frac{1}{s^2}\Sigma_c(s)$ lie inside the pink-colored region when $\Sigma_c(s)$ is "mixed" SNI + strictly passive with $\Sigma_c(0)>0$.

$\frac{c_i}{\varepsilon^2}e^{-j\pi} \to +\infty\angle -\pi$ as $\varepsilon \to 0_+$ and when $\theta = \frac{\pi}{2}$. Similarly, $\overline{\lambda}_i(j0_-) \to +\infty\angle\pi$ when $\theta = -\frac{\pi}{2}$ as the characteristic loci are symmetric about the real axis. However, strictly speaking, $\angle\overline{\lambda}_i(j0_+) > -\pi$ since $\angle\Sigma_c(j0_+) > 0$ and similarly, $\angle\overline{\lambda}_i(j0_-) < +\pi$ as $\angle\Sigma_c(j0_-) < 0$. This hence implies $-\pi < \angle\overline{\lambda}_i(s) < \pi$ when $s \in \Psi_0$. Each locus $\overline{\lambda}_i(j\omega)$ connects the zero-frequency points $\overline{\lambda}_i(j0_-)$ and $\overline{\lambda}_i(j0_+)$ in a CW direction through an almost circular arc having radius $\frac{1}{\varepsilon} \to \infty$ as depicted in Figure 3b. The above analysis guarantees that none of the characteristic loci $\overline{\lambda}_i(j\omega)$ crosses the negative real axis at an infinite distance.

Case II: For the subset $s \in \Psi_{\pm\mathfrak{I}}$ We assume again $\lambda_i[(\mathscr{L}_L + \mathbb{P}) \otimes \Sigma_c(j\omega)] = c_i e^{j\phi_i}$ for every $\omega \in (0, \infty)$. Since $\Sigma_c(s)$ is "mixed" SNI + strictly passive, $\phi_i(\omega) \in \left(-\pi, \frac{\pi}{2}\right)\ \forall \omega \in (0, \infty)$ and hence, for all i, $\angle\overline{\lambda}_i(\mathrm{j}\omega) = (\phi_i - \pi) \in \left(-2\pi, -\frac{\pi}{2}\right)\ \forall \omega \in (0, \infty)$. Following the same logic, we can assert $\angle\overline{\lambda}_i(\mathrm{j}\omega) \in \left(-\frac{3\pi}{2}, 0\right)$ when $\omega \in (-\infty, 0)$. Ultimately, we can conclude that all $\overline{\lambda}_i(j\omega)$ remain inside the pink-colored region shown in Figure 3b when $s \in \Psi_{\pm\mathfrak{I}}$. Note that $\overline{\lambda}_i(j\omega)$ may intersect both negative and/or positive real axes but at finite distances.

Case III: For the subset $s \in \Psi_\infty$ Similar to Case I, for this subset also, we can write

$$\begin{aligned}\overline{\lambda}_i(s)|_{s\in\Psi_\infty} &= \lambda_i[(\mathscr{L}_L + \mathbb{P}) \otimes \Sigma_c(\infty)]\frac{e^{-j2\theta}}{R^2} \\ &= \frac{c_i}{R^2}e^{j(\phi_i - 2\theta)}\end{aligned}$$

upon letting $\lambda_i[(\mathscr{L}_L + \mathbb{P}) \otimes \Sigma_c(\infty)] = c_i e^{j\phi_i}$. Note that $\phi_i = 0$ or $-\frac{\pi}{2}$ or $-\pi$ as $\Sigma_c(\infty)$ cannot be <0 or ≤ 0. Therefore, $\overline{\lambda}_i(+j\infty) = \frac{c_i}{R^2}e^{j\left(\phi_i - \frac{\pi}{2}\right)} \to 0\angle -\frac{\pi}{2}$ or $0\angle -\pi$ or $0\angle -\frac{3\pi}{2}$. Following the same way, we can easily compute the counterpart $\overline{\lambda}_i(-j\infty)$. This then follows that each $\overline{\lambda}_i(j\omega)$ joins the infinite-frequency points $\overline{\lambda}_i(+j\infty)$ and $\overline{\lambda}_i(-j\infty)$ in the CCW direction via a semicircular arc of radius $\frac{1}{R} \to 0$ as illustrated in Figure 3b. The above three cases can be combined to guarantee that all the characteristic loci $\overline{\lambda}_i(s)$ of $T_L(s)$ remain inside the pink-colored area marked in Figure 3b. At the same time, it also ensures that there always exists a finite $\beta^* > 0$ such that the critical point $\left(-\frac{1}{\beta^*} + j0\right)$ is never encircled by any $\overline{\lambda}_i(s)$. This proves the asymptotic stability of the proposed formation-tracking scheme. We will now establish the asymptotic convergence of the formation-tracking error $\xi = \left[\xi_{l_1}\ \ \xi_{l_2}\ \ \cdots\ \ \xi_{l_{N_l}}\right]^\top$. The formation-tracking error dynamics can be obtained from the block diagram in Figure 2 as $\Xi(s) = \left[I + \left((\mathscr{L}_L + \mathbb{P}) \otimes \frac{\beta}{s^2}\Sigma_c(s)\right)\right]^{-1}$. The expression of the time-domain steady-state error can be derived as

$$\begin{aligned}\xi_{ss} &= \lim_{t\to\infty}\xi(t) = \lim_{s\to 0} s\Xi(s) \\ &= \lim_{s\to 0} s\left[I + \left((\mathscr{L}_L + \mathbb{P}) \otimes \tfrac{\beta}{s^2}\Sigma_c(s)\right)\right]^{-1}\hat{\mathbf{R}}(s) \\ &\quad \left[\text{denoting } \hat{\mathbf{r}} = \mathbf{r} + \mathbf{h} \text{ and } \hat{\mathbf{R}}(s)\right. \\ &\quad \left.= \text{Laplace of } \hat{\mathbf{r}}\right] \\ &= \lim_{s\to 0} s^2[s^2 I + ((\mathscr{L}_L + \mathbb{P}) \otimes \beta\Sigma_c(s))]^{-1}\left(s\hat{\mathbf{R}}(s)\right) \\ &= [(\mathscr{L}_L + \mathbb{P}) \otimes \beta\Sigma_c(0)]^{-1}\left(\lim_{s\to 0} s^2 I\right) \\ &\quad \times \left(\lim_{s\to 0} s[\mathbf{R}(s) + \mathbf{h}(s)]\right) = [0\ 0 \cdots 0]^\top\end{aligned}$$

since $\Sigma_c(0) > 0$, $(\mathscr{L}_L + \mathbb{P}) > 0$ and $\mathbf{r}(t)$ and $\mathbf{h}(t)$ all are bounded signals for all $t \geq 0$. This hence implies $\mathbf{y} \to (\mathbf{r} + \mathbf{h})$ at the steady-state. This completes the proof.

Part II: Containment of N_f follower UAVs Proceeding along the same direction as exercised in Part I, the asymptotic stability of the containment control scheme (the lower block diagram in Figure 2) for the followers can be readily established along with $\lim_{t\to\infty}\zeta(t) = 0$ where ζ denotes the containment error. This implies $\lim_{t\to\infty}\left(\mathscr{L}_F\mathbf{y}_f + \mathscr{L}_{FL}\mathbf{y}_l\right) = 0 \Leftrightarrow$ $\lim_{t\to\infty}\left(\mathbf{y}_f + \mathscr{L}_F^{-1}\mathscr{L}_{FL}\mathbf{y}_l\right) = 0 \Leftrightarrow$ $\lim_{t\to\infty}\left(y_{f_k} - \sum_{j=1}^{N_l}\alpha_{kj}y_{l_j}\right) = 0$ for all $k \in \{1,2,\ldots,N_f\}$ where $\mathbf{y}_l = \left[y_{l_1}\ \ y_{l_2}\ \ \cdots\ \ y_{l_{N_l}}\right]^\top$, $\mathbf{y}_f = \left[y_{f_1}\ \ y_{f_2}\ \ \cdots\ \ y_{f_{N_f}}\right]^\top$ and $\sum_{j=1}^{N_l}\alpha_{kj} = 1$ with $\alpha_{kj} > 0$ since each row sum of the matrix $-\mathscr{L}_F^{-1}\mathscr{L}_{FL}$ is equal to 1. This means that all followers will

be driven inside a convex hull spanned by the coordinates of the leaders. Note that $\mathscr{L}_F^{-1}$ exists because $\mathscr{L}_F > 0$ via Property 3. This completes the proof. □

Remark 1. In contrast to many existing FCC schemes that rely on the Lyapunov stability approach [19, 22, 23, 38, 39], our method exploits the characteristic loci property of networked NI and SNI systems to prove the convergence of the formation-tracking and containment errors. Therefore, the proposed methodology does not need to search for an appropriate Lyapunov candidate function and is free from a complicated and long chain of proof. In addition, our method relies only on output feedback, making it a better choice when full-state measurement is not possible. Besides, the proposed "mixed" SNI + strictly passive control law does not use any nonlinear control term, unlike the literature [19, 33–37]. Hence, it does not suffer any chattering effect.

Remark 2. The proposed FCC scheme introduces a novel approach for implementing formation-tracking among leader agents in both static and time-varying formation configurations. Moreover, the proposed scheme provides a straightforward extension to tackle the complexities of a multi-group formation-tracking problem by incorporating multiple targets for tracking and accommodating multiple subgroups within the communication topology.

5 | MATLAB SIMULATION RESULTS

The Matlab simulation case study presented in this section compares the performance of the proposed FCC scheme, which utilizes a distributed "mixed" SNI + strictly passive controller, with that of an SNI-only FCC scheme adopted from previous works [10, 11]. We considered a 3D formation-containment control problem for a group of UAV agents whose translational dynamics can be modeled as a networked double integrator agent. The group consists of eight leaders and eight followers. Figure 4 describes the interactions among the leader and follower agents. In this figure, Label "0" denotes the virtual target; Labels 1–8 indicate the leaders, and Labels 9–16 denote the followers. The main control objective was to attain a 3D cubic formation by the leaders, while the followers were expected to converge inside a convex hull spanned by the leaders. We selected a "mixed" SNI + strictly passive controller $\Sigma_c(s) = \frac{s+0.01}{s^2+50s+500}(s+40)$ to be fit into the outer loop of the proposed scheme. At the same time, an SNI-only controller $C(s) = -\frac{s+1}{s+100}$ was taken for a comparative study.

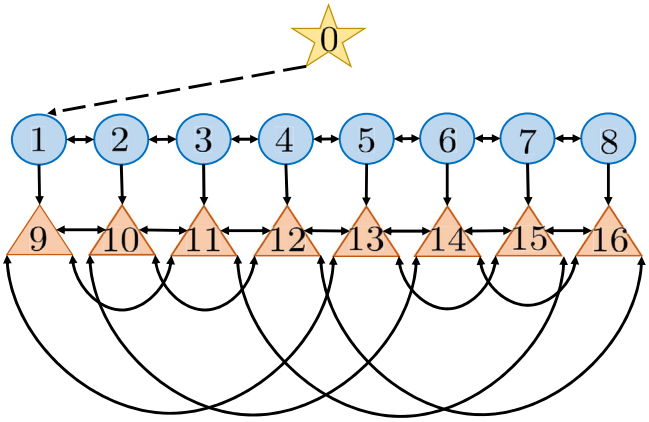

FIGURE 4 The communication topology used in the simulation case study.

Figure 5a shows the initial orientation of all the participating agents. Figure 5b shows that the eight leaders have successfully achieved the desired 3D cubic formation, and the followers have converged inside the convex hull spanned by the leaders under the influence of the proposed "mixed" SNI and strictly passive FCC scheme. In these figures, The red stars mark the positions of the virtual target. Figure 6 compares the 2-norms of the formation-tracking errors of the leaders (in Figure 6a) and containment errors of the followers (in Figure 6b), simulated by applying respectively the proposed FCC scheme and an SNI-only FCC scheme adopted from the literature [10, 11]. In the case of the proposed FCC scheme, we observe that the formation-tracking and containment errors decayed to zero within 5 s only (see Figure 6a). But in the case of the SNI-only FCC scheme, the errors decayed to zero after 20 s with some inaccuracies, as reported in Figure 6b. The comparative study reveals that the proposed "mixed" SNI + strictly passive FCC scheme offers a better steady-state and dynamic performance than the SNI-only FCC scheme adopted from previous works [10, 11].

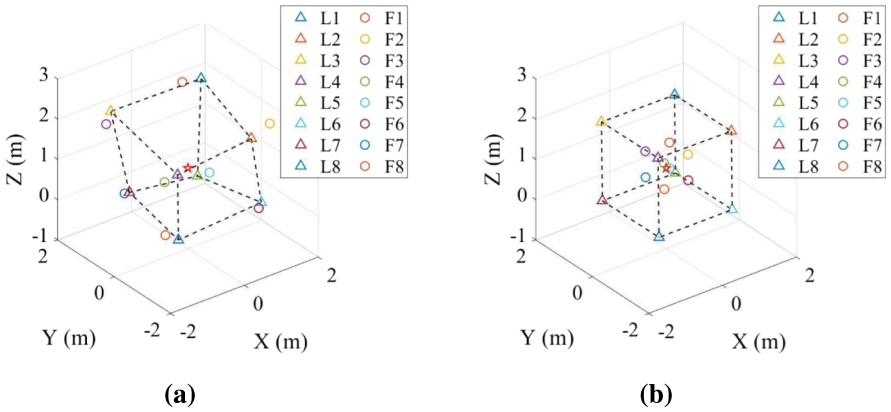

FIGURE 5 [Simulation results]. (a) Initial orientation of the UAV agents at $t = 0$ s. (b) At $t = 5$ s, the leaders attained the desired cubic formation, and the followers entered into the convex hull spanned by the leaders.

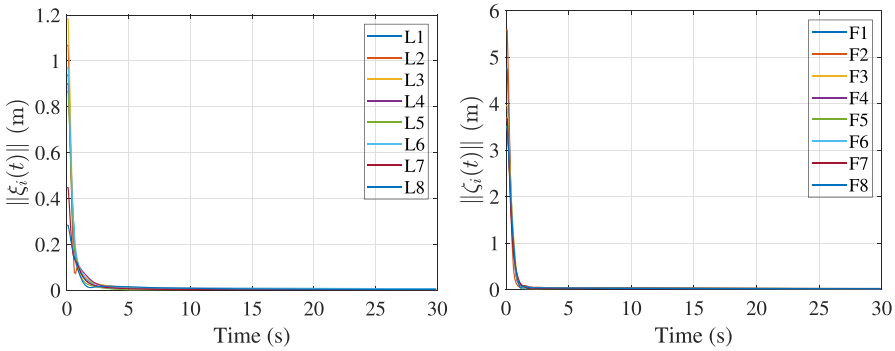

(a) The proposed FCC scheme based on a 'mixed' SNI + Strictly Passive controller in this paper.

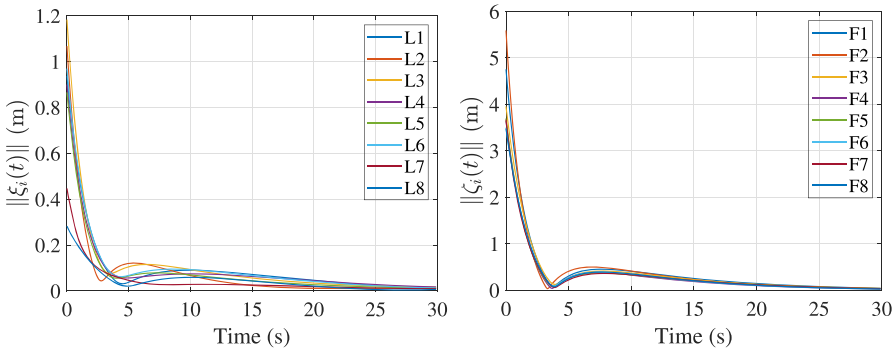

(b) The pure SNI controller from articles [10, 11].

FIGURE 6 [Performance comparison study]. Comparison of the 2-norms of the (i) formation-tracking errors $\|\xi_i(t)\|$ of the leaders and (ii) the containment errors $\|\zeta_i(t)\|$ of the followers, simulated by applying the proposed FCC scheme and an SNI-only FCC scheme adopted from previous works [10, 11].

6 | EXPERIMENTAL VALIDATION RESULTS

The proposed dynamic output feedback FCC scheme was implemented on a fleet of Crazyflie 2.1 quadcopters [46] for validation purposes. A "mixed" SNI + strictly passive controller transfer function was chosen to conduct two indoor multi-UAV experiments aiming for a formation-containment operative and a time-varying formation-tracking mission. The experimental results demonstrate the feasibility of the scheme and show its potential applications. A recorded video clip of the experiments can be found in the supplementary material and at https://youtu.be/grq0LWp6b98.

6.1 | Experimental setup

Figure 7a shows the components of a Crazyflie 2.1 nano quadcopter with some expansion decks. The Crazyflie is a small-size (with a diagonal length of 92 mm from motor to motor) and lightweight (about 27 g) quadcopter

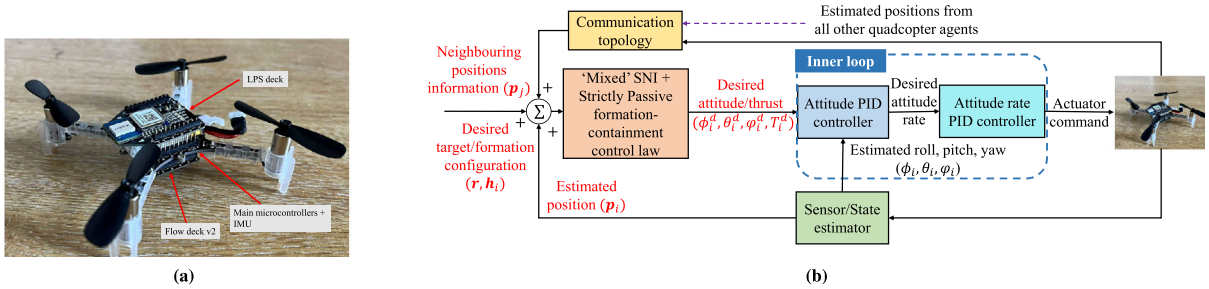

FIGURE 7 (a) A Crazyflie 2.1 nano quadcopter. (b) The proposed two-loop control configuration implemented in the experiments for each of the UAVs to achieve formation/containment.

developed as an open-source UAV-test platform by Bitcraze Pvt. Ltd. [46]. The Crazyflie quadcopters can be equipped with additional decks, such as Flow Deck v2 and Loco-Positioning System (LPS) Deck, to enable autonomous flight experiments. The LPS provides the absolute position coordinates of a flying UAV with an accuracy of 0.1 m.

Figure 7b depicts the two-loop control configuration implemented in the flight experiments for each UAV to achieve the formation-containment control objective. The inner loop employs a cascaded PID attitude controller to render the closed-loop translational dynamics of a UAV into a double integrator system. At the same time, a "mixed" SNI + strictly passive distributed controller operates on the inner-closed-loop double integrator dynamics and plays the role of FCC. The position of each quadcopter is transmitted to the base station, and the control command is generated through the base station and sent to each quadcopter via Crazyradio dongles [46]. However, if each quadcopter can directly measure the relative positions of others or share its position with its neighbors via Bluetooth or Wi-Fi, the base station can be easily removed.

6.2 | Modeling of the UAVs

The dynamics of small and lightweight quadcopter UAVs, such as Crazyflie nano quadcopter, can be represented by the following Newton-Euler equations:

$$\begin{cases} m\ddot{\mathbf{p}} = -mg\mathbf{e}_z + \mathbf{R}_e^b(\eta)\mathbf{F}_b, \\ \mathbf{I}\dot{\omega} = -\omega \times \mathbf{I}\omega + \tau_b, \end{cases} \tag{7}$$

where $\mathbf{p} = [x,y,z]^\top$ and $\omega = [p,q,r]^\top$ are the position vector in the earth frame and the angular velocity vector in the body frame. $m \in \mathbb{R}$ and $\mathbf{I} \in \mathbb{R}^{3\times 3}$ are the mass and the inertia matrix of a quadcopter UAV. $\mathbf{F}_b = [0,0,T]^\top$ and τ_b are the total force vector and the total drag torque vector acting on the quadcopter UAV with respect to the body frame. T is the total thrust produced by the four rotors. g is the gravity constant, and $\mathbf{e}_z = [0,0,1]^\top$ is the unit vector with respect to the earth frame. Following the $Z-Y-X$ Euler rotation sequence, the rotation matrix for transforming a vector from the body frame to the earth (inertial) frame is given by

$$\mathbf{R}_e^b(\eta) = \begin{bmatrix} c\theta c\psi & s\phi s\theta c\psi - c\phi s\psi & c\phi s\theta c\psi + s\phi s\psi \\ c\theta s\psi & s\phi s\theta s\psi + c\phi c\psi & c\phi s\theta s\psi - s\phi c\psi \\ -s\theta & s\phi c\theta & c\phi c\theta \end{bmatrix} \tag{8}$$

where $\eta = [\phi,\theta,\psi]^\top$ are the Euler angles, $c\phi = \cos\phi$ and $s\phi = \sin\phi$. The relation between the angular velocity and the derivatives of the Euler angles can be expressed as

$$\begin{bmatrix} p \\ q \\ r \end{bmatrix} = \begin{bmatrix} 1 & 0 & -\sin\theta \\ 0 & \cos\phi & \sin\phi\cos\theta \\ 0 & -\sin\phi & \cos\phi\cos\theta \end{bmatrix} \begin{bmatrix} \dot{\phi} \\ \dot{\theta} \\ \dot{\psi} \end{bmatrix}. \tag{9}$$

Remark 3. Due to the different time scales of translational and attitude dynamics of a quadcopter UAV, hovering and maneuvering can be controlled separately by a two-loop control configuration shown in Figure 7b (see previous works [20, 47] and the references therein). To achieve the formation-containment and tracking behaviors, a distributed "mixed" SNI + strictly passive controller is implemented in the outer loop and generates the virtual control input $\mathbf{u} = [u_x,u_y,u_z]^\top$. The virtual control input is then transformed into the desired thrust (T^d), roll angle (ϕ^d), and pitch angle (θ^d), that is,

$$\begin{cases} T^d = m\sqrt{u_x^2+u_y^2+(u_z+g)^2}, \\ \phi^d = \sin^{-1}\left(m\dfrac{u_x\sin\psi_d - u_y\cos\psi_d}{T}\right), \\ \theta^d = \tan^{-1}\left(\dfrac{u_x\cos\psi_d - u_y\sin\psi_d}{u_z+g}\right), \end{cases} \tag{10}$$

where (ψ_d) is the desired yaw angle predefined by the user.

According to Remark 3, the closed-loop translational dynamics of a quadcopter UAV can be approximated by a decoupled three-input-three-output double integrator system $\ddot{\mathbf{p}}_i = \mathbf{u}_i$, where $\mathbf{p}_i = [x_i, y_i, z_i]^\top$ and $\mathbf{u}_i = [u_{x_i}, u_{y_i}, u_{z_i}]^\top$ denote the position and virtual control input vector of the ith quadcopter UAV.

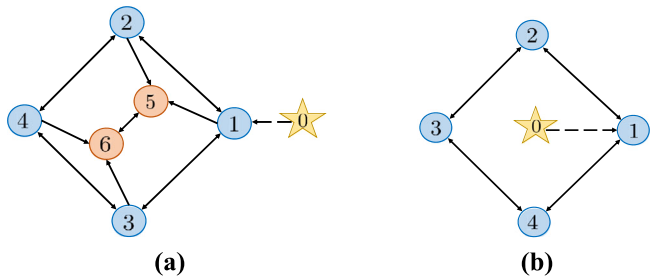

FIGURE 8 (a) The communication topology used in Experiment 1. (b) The topology used in Experiment 2.

6.3 | Experiment 1: A formation-containment mission

In Experiment 1, we deploy a group of six Crazyflie quadcopters connected via a network of four leaders and two followers to perform a formation-containment mission. In the beginning, the leaders were scattered at the center of the flight arena, while the followers were placed at the top right corner (far from the convex hull spanned by those leaders), as shown in Figure 9a. The objective of the leader agents was to achieve a diamond-shaped formation, and the followers were supposed to converge into a convex hull spanned by the leaders. We selected a "mixed" SNI + strictly passive controller $\Sigma_c(s) = \frac{s+1}{(s^2+10s+200)(s+40)}$, with $\beta = 200$, to implement as the outer-loop controllers of the proposed FCC scheme. The communication topology between the leader and follower quadcopters is described by Figure 8a. Label "0" denotes the virtual target; Labels 1–4 denote the leaders, and Labels 5 and 6 indicate the followers.

Figure 9 shows the snapshots of an indoor multi-UAV experiment on achieving a formation-containment mission. The time-evolvement of the trajectories is also shown on the X-Y plane. Figure 9b depicts that four

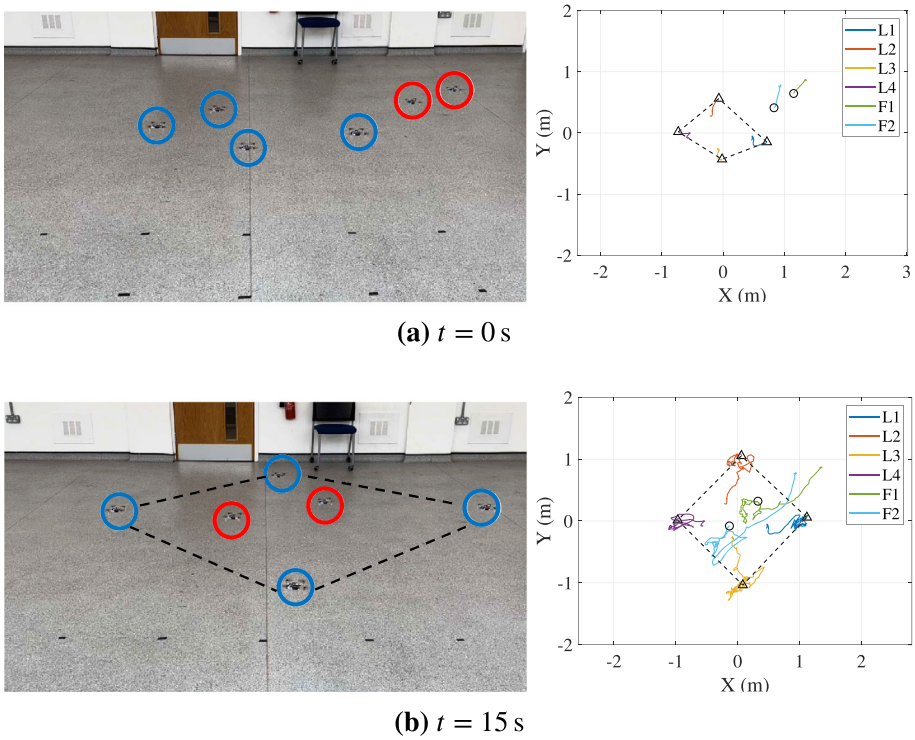

FIGURE 9 [Results for Experiment 1]. (a) Initial orientation of the leader and follower UAV agents at $t = 0$ s. (b) At $t = 15$ s, a diamond-shaped formation was attained by the leaders and the followers converged into the convex hull spanned by those leaders. In the snapshot (left ones), the blue and red circles mark the leaders and followers, respectively.

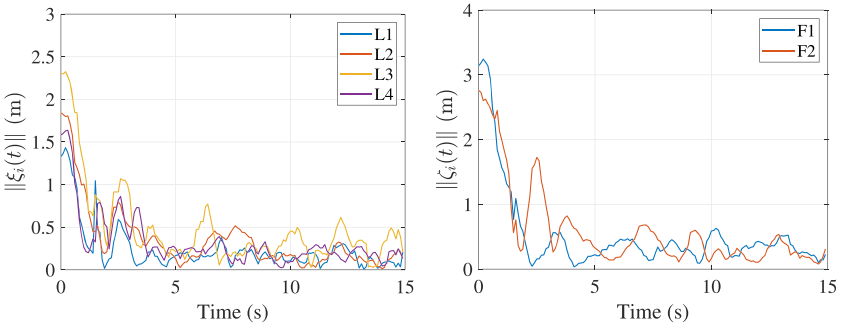

FIGURE 10 [Results for Experiment 1]. (a) The 2-norm of the formation-tracking errors $\|\xi_i(t)\|$ of the leaders. (b) The 2-norm of the containment errors $\|\zeta_i(t)\|$ of the followers. Note that the position sensing accuracy of the LPS is around 0.1 m.

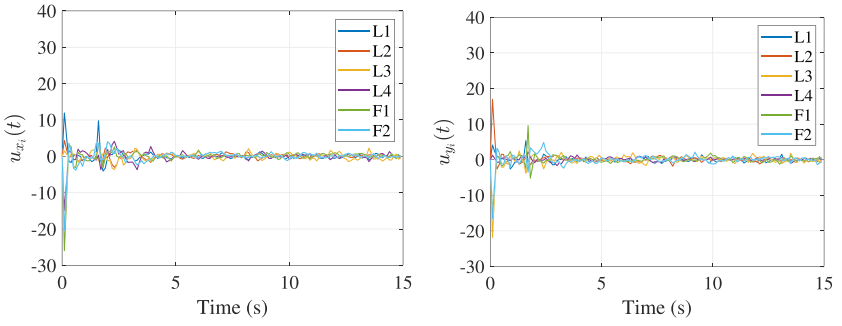

FIGURE 11 [Results for Experiment 1]. (a) The X-axis component of the demanded control effort by each UAV. (b) The Y-axis component of the demanded control effort.

leader agents attained the desired diamond-shaped formation and, at the same time, the two followers entered and converged into the convex hull spanned by the leaders' positions. In addition, Figure 10a,b portrays the 2-norms of the formation-tracking and containment errors of the agents, revealing that the errors decayed almost to zero within a few seconds only. The X and Y components of the demanded control efforts by the UAVs, computed from (4) and (5), are reported in Figure 11a and Figure 11b, respectively. All these experimental validation results conclude that the group of six Crazyflie 2.1 nano quadcopter UAVs accomplished the formation-containment objective under the influence of the proposed dynamic output feedback FCC scheme that implements a distributed "mixed" SNI + strictly passive controller $\Sigma_c(s)$.

6.4 | Experiment 2: A circular time-varying formation-tracking mission

In Experiment 2, four Crazyflie quadcopters, connected via a graph, were deployed to perform a time-varying formation-tracking mission. During the first 25 s, the quadcopters would attain a circular time-varying formation surrounding a static virtual target. In between 25–40 s, the whole formation assembly of the quadcopters must undergo a translational maneuver to track the moving virtual target without disturbing the formation shape. In Experiment 2, the virtual target had a velocity of 0.2 m/sec along the X-axis. The formation configuration vectors $\mathbf{h}_i$ for the agents to obtain a circular time-varying formation are noted below:

$$\mathbf{h}_i(t) = \begin{bmatrix} \cos\left(0.02t + \frac{2(i-1)\pi}{4}\right) \\ \sin\left(0.02t + \frac{2(i-1)\pi}{4}\right) \end{bmatrix} \quad \forall i \in \{1,2,...,4\}.$$

A "mixed" SNI + strictly passive controller $\Sigma_c(s) = \frac{s+1}{(s^2+10s+200)(s+40)}$, with $\beta = 200$, was chosen to be implemented in the outer-loop control. The communication topology among the leader and follower UAV agents, including the virtual target, has been portrayed in Figure 8b.

Figure 12 depicts the snapshots of the second multi-UAV experiment on a time-varying formation-tracking mission. Four UAV agents participated in this experiment and attained a desired circular time-varying formation while tracking a moving virtual target (marked by a Red star). Figure 13a plots the trajectories of all the UAV agents and the virtual target. The initial and final positions of the agents were marked by circles and triangles,

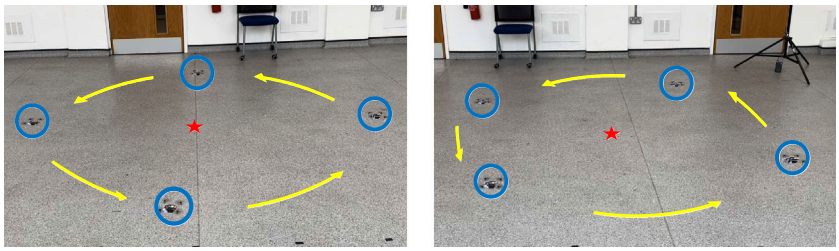

(a) (b)

FIGURE 12 [Results for Experiment 2]. (a) At 20 s, all four UAV agents achieved a circular time-varying formation surrounding a static virtual target (marked by a red star). (b) The figure shows (at $t = 35$ s) the time-varying formation-tracking was maintained even when the virtual target moved from its initial location.

FIGURE 13 [Results for Experiment 2]. (a) Four UAV agents attained the desired circular time-varying formation starting from an arbitrary initial location. The time evolvement of the spatial trajectories of the UAV agents is also shown. (b) The 2-norms of the formation-tracking errors $\|\xi_i(t)\|$ of the agents.

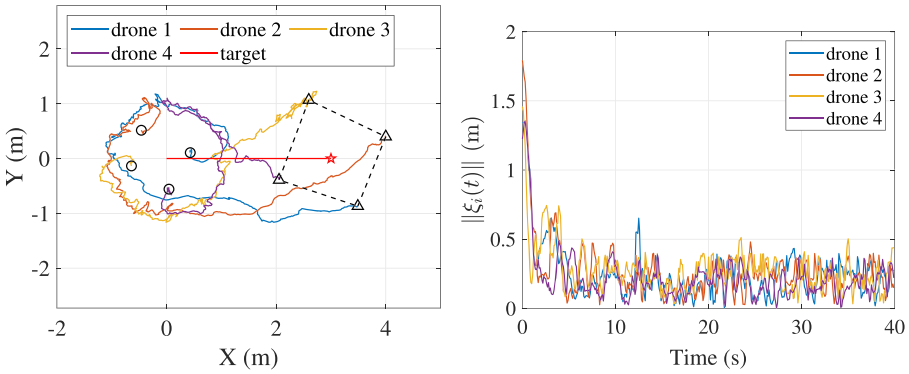

(a) (b)

FIGURE 14 [Results for Experiment 2]. (a) The X-axis components of the control efforts demanded by the UAVs. (b) The Y-axis components of the demanded control efforts.

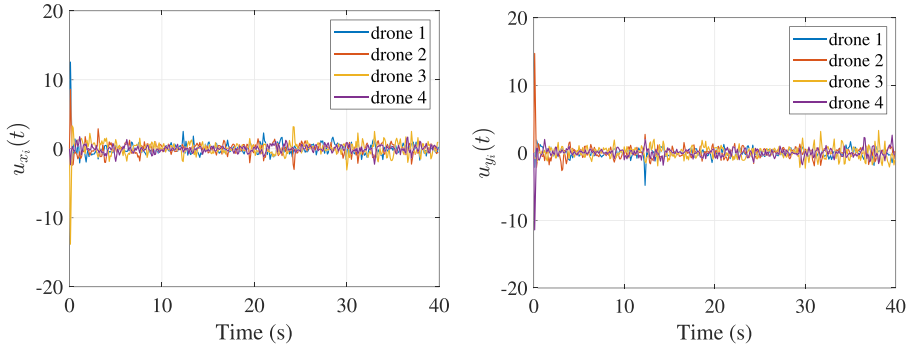

(a) (b)

respectively. Figure 13b reports that the 2-norms of the formation-tracking errors of the UAVs converged nearly to zero within a few seconds only. Note that the positional accuracy of the LPS is around 0.1 m. Figure 14a and Figure 14b portray the X and Y components of the control efforts demanded by the UAV agents during the formation-tracking mission. These experimental validation results confirm the feasibility and effectiveness of the proposed distributed "mixed" SNI + strictly passive FCC scheme.

7 | CONCLUSIONS

The article dealt with the properties of interconnected NI systems and extended the results to networked multi-agent systems (MASs) that exhibit NI/SNI properties. A dynamic output feedback formation-containment control (FCC) scheme has been designed for a double-integrator MAS that inherently satisfies the NI property. The main motivation was that many robotic systems and autonomous vehicles (e.g., a class of UAVs and UGVs) could be

modeled as or feedback-linearized into a double integrator. Then, a distributed SNI controller can be conveniently designed for NI MASs to achieve cooperative control objectives with moderate time-domain performance. This paper has investigated that a "mixed" SNI + strictly passive cooperative control scheme improves steady-state and dynamic performance. Unlike the existing Lyapunov theory-based cooperative control schemes, the proposed one has exploited the Characteristic Loci technique to prove the stability of the tracking error dynamics. It has significantly reduced the mathematical complexity and facilitated easy implementation. An in-depth Matlab simulation case study accompanied by experimental validation results (conducted on a fleet of Crazyflie 2.1 nano quadcopters [46]) demonstrates the feasibility and performance of the proposed FCC scheme. However, it is noted that the proposed FCC scheme is only applicable to single/double integrator NI agents, and selecting the appropriate controller for the scheme may necessitate the expertise and experience of a control engineer. In the future, obstacle-avoidance controllers could be designed using improved artificial potential function algorithms [48].

AUTHOR CONTRIBUTIONS

Yu-Hsiang Su: Conceptualization; data curation; formal analysis; investigation; methodology; software; validation; visualization; writing—original draft; writing—review and editing. **Parijat Bhowmick:** Conceptualization; formal analysis; funding acquisition; methodology; project administration; supervision; writing—original draft; writing—review and editing. **Alexander Lanzon:** Funding acquisition; project administration; supervision; writing—review and editing.

CONFLICT OF INTEREST STATEMENT

The authors declare no potential conflict of interests.

ORCID

Yu-Hsiang Su https://orcid.org/0000-0002-5208-714X
Parijat Bhowmick https://orcid.org/0000-0003-3127-8892
Alexander Lanzon https://orcid.org/0000-0003-3424-8808

REFERENCES

1. A. Lanzon and I. R. Petersen, *Stability robustness of a feedback interconnection of systems with negative imaginary frequency response*, IEEE Trans. Autom. Control **53** (2008), no. 4, 1042–1046.
2. C. A. Desoer and M. Vidyasagar, *Feedback systems: Input-output properties*, Classics in Applied Mathematics, Society for Industrial and Applied Mathematics, 2009.
3. J. L. Fanson and T. K. Caughey, *Positive position feedback control for large space structures*, AIAA J. **28** (1990), no. 4, 717–724.
4. B. Bhikkaji, S. O. Reza Moheimani, and I. R. Petersen, *A negative imaginary approach to modeling and control of a collocated structure*, IEEE/ASME Trans. Mechatron. **17** (2012), no. 4, 717–727.
5. D. Angeli, *Systems with counterclockwise input-output dynamics*, IEEE Trans. Autom. Control **51** (2006), no. 7, 1130–1143.
6. A. J. van der Schaft, Positive feedback interconnection of hamiltonian systems, Proceedings of 50th IEEE Conference on Decision and Control and European Control Conference, 2011, pp. 6510–6515.
7. P. Bhowmick and A. Lanzon, Time-domain output negative imaginary systems and its connection to dynamic dissipativity, Proceedings of 59th IEEE Conference on Decision and Control, 2020, pp. 5167–5172.
8. A. Lanzon and P. Bhowmick, *Characterisation of input-output negative imaginary systems in a dissipative framework*, IEEE Trans. Autom. Control **68** (2023), no. 2, 959–974.
9. M. A. Mabrok, A. G. Kallapur, I. R. Petersen, and A. Lanzon, *Generalizing negative imaginary systems theory to include free body dynamics: Control of highly resonant structures with free body motion*, IEEE Trans. Autom. Control **59** (2014), no. 10, 2692–2707.
10. P. Bhowmick, A. Ganguly, and S. Sen, *A new consensus-based formation tracking scheme for a class of robotic systems using negative imaginary property*, IFAC-PapersOnLine **55** (2022), no. 1, 685–690.
11. J. Hu, B. Lennox, and F. Arvin, *Robust formation control for networked robotic systems using Negative Imaginary dynamics*, Automatica **140** (2022), 1–9.
12. O. Skeik, J. Hu, F. Arvin, and A. Lanzon, Cooperative control of integrator negative imaginary systems with application to rendezvous multiple mobile robots, Proceedings of the 12th IEEE International Workshop on Robot Motion and Control, Poznan, Poland, 2019, pp. 15–20.
13. J. Wang, A. Lanzon, and I. R. Petersen, *Robust output feedback consensus for networked negative-imaginary systems*, IEEE Trans. Autom. Control **60** (2015), no. 9, 2547–2552.
14. N. Nikooienejad and S. O. Reza Moheimani, *Convex synthesis of SNI controllers based on frequency-domain data: MEMS nanopositioner example*, IEEE Trans. Control Syst. Technol. **30** (2022), no. 2, 767–778.
15. J. Xiong, I. R. Petersen, and A. Lanzon, *A negative imaginary lemma and the stability of interconnections of linear negative imaginary systems*, IEEE Trans. Autom. Control **55** (2010), no. 10, 2342–2347.
16. A. Ferrante, A. Lanzon, and L. Ntogramatzidis, *Foundations of not necessarily rational negative imaginary systems theory: Relations between classes of negative imaginary and positive real systems*, IEEE Trans. Autom. Control **61** (2016), no. 10, 3052–3057.
17. A. Ferrante and L. Ntogramatzidis, *Some new results in the theory of negative imaginary systems with symmetric transfer matrix function*, Automatica **49** (2013), no. 7, 2138–2144.
18. A. Lanzon and H.-J. Chen, *Feedback stability of negative imaginary systems*, IEEE Trans. Autom. Control **62** (2017), no. 11, 5620–5633.

19. Z. Li and Z. Duan, *Cooperative control of multi-agent systems: A consensus region approach*, 1st ed., CRC Press, 2014.
20. Y.-H. Su and A. Lanzon, Formation-containment tracking and scaling for multiple quadcopters with an application to choke-point navigation, Proceedings of the IEEE International Conference on Robotics and Automation, IEEE, Philadelphia, PA, USA, 2022, pp. 4908–4914.
21. H. Liu, L. Cheng, M. Tan, Z. Hou, Z. Cao, and M. Wang, Containment control with multiple interacting leaders under switching topologies, Proceedings of the 32nd Chinese Control Conference, Xian, China, 2013, pp. 7093–7098.
22. L. M. Chen, C. J. Li, J. Mei, and G. F. Ma, *Adaptive cooperative formation–containment control for networked Euler-Lagrange systems without using relative velocity information*, IET Control Theory Appl. **11** (2017), no. 9, 1450–1458.
23. L. Chen, J. Mei, C. Li, and G. Ma, *Distributed leader-follower affine formation maneuver control for high-order multiagent systems*, IEEE Trans. Autom. Control **65** (2020), no. 11, 4941–4948.
24. H. Liang, L. Chen, Y. Pan, and H.-K. Lam, *Fuzzy-based robust precision consensus tracking for uncertain networked systems with cooperative–antagonistic interactions*, IEEE Trans. Fuzzy Syst. **31** (2023), no. 4, 1362–1376.
25. H. Liang, Z. Du, T. Huang, and Y. Pan, *Neuroadaptive performance guaranteed control for multiagent systems with power integrators and unknown measurement sensitivity*, IEEE Trans. Neural Netw. Learn. Syst. (2022), 1–12.
26. Y.-H. Su, P. Bhowmick, and A. Lanzon, *A robust adaptive formation control methodology for networked multi-UAV systems with applications to cooperative payload transportation*, Control Eng. Pract. **138** (2023), 105608.
27. D. Abara, P. Bhowmick, and A. Lanzon, Cooperative control of multi-tilt tricopter drones applying a 'mixed' negative imaginary and strict passivity technique, 2023 European Control Conference (ECC), IEEE, Bucharest, Romania, 2023.
28. Y.-H. Su, P. Bhowmick, and A. Lanzon, A Negative Imaginary Theory-Based Time-Varying Group Formation Tracking Scheme for Multi-Robot Systems: Applications to Quadcopters, 2023 IEEE International Conference on Robotics and Automation (ICRA), IEEE, London, United Kingdom, 2023, pp. 1435–1441.
29. Y.-H. Su, P. Bhowmick, and A. Lanzon, Cooperative Control of Multi-Agent Negative Imaginary Systems with Applications to UAVs, Including Hardware Implementation Results, 2023 European Control Conference (ECC), IEEE, Bucharest, Romania, 2023.
30. J. Wang, A. Lanzon, and I. R. Petersen, *Robust cooperative control of multiple heterogeneous negative-imaginary systems*, Automatica **61** (2015), 64–72.
31. V. P. Tran, M. A. Garratt, and I. R. Petersen, *Multi-vehicle formation control and obstacle avoidance using negative-imaginary systems theory*, IFAC J. Syst. Control **15** (2021), no. 100117, 1–23.
32. P. Bhowmick and S. Patra, *On decentralized integral controllability of stable negative-imaginary systems and some related extensions*, Automatica **94** (2018), 443–451.
33. J. Hu, P. Bhowmick, and A. Lanzon, *Distributed adaptive time-varying group formation tracking for multi-agent systems with multiple leaders on directed graphs*, IEEE Trans. Control Netw. Syst. **7** (2020), no. 1, 140–150.
34. J. R. Klotz, T.-H. Cheng, and W. E. Dixon, *Robust containment control in a leader-follower network of uncertain Euler-Lagrange systems*, Int. J. Robust Nonlin. Control **26** (2016), no. 17, 3791–3805.
35. Z. Li, Z. Duan, W. Ren, and G. Feng, *Containment control of linear multi-agent systems with multiple leaders of bounded inputs using distributed continuous controllers*, Int. J. Robust Nonlin. Control **25** (2015), no. 13, 2101–2121.
36. J. Mei, W. Ren, and G. Ma, *Distributed containment control for Lagrangian networks with parametric uncertainties under a directed graph*, Automatica **48** (2012), no. 4, 653–659.
37. C. Wang, H. Tnunay, Z. Zuo, B. Lennox, and Z. Ding, *Fixed-time formation control of multirobot systems: Design and experiments*, IEEE Trans. Industr. Electron. **66** (2019), no. 8, 6292–6301.
38. X. Dong, Y. Hua, Y. Zhou, Z. Ren, and Y. Zhong, *Theory and experiment on formation-containment control of multiple multirotor unmanned aerial vehicle systems*, IEEE Trans. Autom. Sci. Eng. **16** (2019), no. 1, 229–240.
39. J. Hu, P. Bhowmick, I. Jang, F. Arvin, and A. Lanzon, *A decentralized cluster formation containment framework for multirobot systems*, IEEE Trans. Robot. **37** (2021), no. 6, 1936–1955.
40. W. Jiang, G. Wen, Z. Peng, T. Huang, and A. Rahmani, *Fully distributed formation-containment control of heterogeneous linear multiagent systems*, IEEE Trans. Autom. Control **64** (2019), no. 9, 3889–3896.
41. P. Bhowmick, H.-J. Chen, and A. Lanzon, Properties of positive feedback interconnected negative imaginary systems, Proceedings of 13th Asian Control Conference, Jeju Islands, South Korea, 2022, pp. 2310–2315.
42. S. Patra and A. Lanzon, *Stability analysis of interconnected systems with 'mixed' negative-imaginary and small-gain properties*, IEEE Trans. Autom. Control **56** (2011), no. 6, 1395–1400.
43. S. K. Das, H. R. Pota, and I. R. Petersen, Stability analysis for interconnected systems with 'mixed' passivity, negative-imaginary and small-gain properties, Proceedings of Australian Control Conference, 2013, pp. 201–206.
44. J. J. Belletrutti and A. G. J. MacFarlane, *Characteristic loci techniques in multivariable-control-system design*, Proc. Instit. Electr. Eng. **118** (1971), no. 9, 1291–1297.
45. A. G. J. Macfarlane and J. J. Belletrutti, *The characteristic locus design method*, Automatica **9** (1973), no. 5, 575–588.
46. Bitcraze. https://www.bitcraze.io
47. F. Kendoul, *Nonlinear hierarchical flight controller for unmanned rotorcraft: design, stability, and experiments*, J. Guid. Control Dyn. **32** (2009), no. 6, 1954–1958.
48. S. Xie, J. Hu, P. Bhowmick, Z. Ding, and F. F. Arvin, *Distributed motion planning for safe autonomous vehicle overtaking via artificial potential field*, IEEE Trans. Intell. Transport. Syst. **23** (2022), no. 11, 21531–21547.

AUTHOR BIOGRAPHIES

Yu-Hsiang Su received his BS degree in mechanical engineering from National Chiao Tung University in Hsinchu, Taiwan, in 2017, and his MS degree in advanced control and systems engineering from the University of Manchester, UK, in 2019. He is currently pursuing a PhD degree in electrical and electronic engineering at the University of Manchester, UK. His research interests include cooperative control of multi-agent systems and their applications.

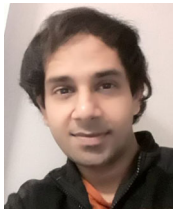

Parijat Bhowmick is presently an assistant professor at the Department of EEE of IIT Guwahati, India. Before joining this position, he worked as a post-doctoral research associate at the Control Systems Centre, University of Manchester, for 3 years. He completed his PhD degree in control engineering from IIT Kharagpur, India, in the year 2018. He did his master's from Jadavpur University in 2012 with the same specialization. He was a recipient of the University Gold Medal in his masters and was also a recipient of the Institute Silver Medal during his bachelors. He is an active researcher in the horizon of robust control of uncertain systems, negative imaginary systems theory, vibration control of mechatronic systems, cooperative control of multi-agent systems (including multi-agent systems), and control of smart/micro-grid Systems.

Alexander Lanzon received his PhD degree in control engineering and his MPhil degree in robot control from the University of Cambridge, Cambridge, UK, in 2000 and 1997, respectively, and received his BEng (Hons) degree in electrical and electronic engineering from the University of Malta, Msida, Malta, in 1995. He has held research and academic positions at Georgia Institute of Technology, Atlanta GA, USA, and the Australian National University, Canberra ACT, Australia, and industrial positions at ST-Microelectronics Ltd., Kirkop, Malta; Yaskawa Denki (Tokyo) Ltd., Saitama-Ken, Japan; and National ICT Australia Ltd., Canberra ACT, Australia. In 2006, he joined the University of Manchester, Manchester, UK, where he now holds the Chair in Control Engineering. His research interests include the fundamentals of feedback control theory, negative imaginary systems theory, robust control theory, input-output nonlinear control theory, and applying robust and nonlinear control theory to innovative mechatronic, robotic, and drone applications. He is a fellow of the Institute of Mathematics and its Applications, the Institute of Measurement and Control and the Institution of Engineering and Technology. He is currently an associate editor of the IEEE Control Systems Letters (L-CSS). He has served as an associate editor of the IEEE Transactions on Automatic Control from 2012 to 2018, and as a subject editor of the International Journal of Robust and Nonlinear Control from 2012 to 2015.

SUPPORTING INFORMATION

Additional supporting information can be found online in the Supporting Information section at the end of this article.

How to cite this article: Y.-H. Su, P. Bhowmick, and A. Lanzon, *Properties of interconnected negative imaginary systems and extension to formation-containment control of networked multi-UAV systems with experimental validation results*, Asian J. Control **27** (2025), 99–116. DOI 10.1002/asjc.3258